Strict Sliding Mode Control with Power Reaching Law and Disturbance Bounds in Synchronous Servo Tracking Drive System

Quoc Huy Vu
Control, Automation in Production and Improvement of Technology Institute (CAPITI), Hanoi, Vietnam
Email: maihuyvu@gmail.com (Q.H.V.), vuquochuy@capiti.info (Q.H.V.)

***Abstract*—This paper presents the analysis and synthesis results of a sliding mode controller for tracking drive systems using a synchronous servo motor and its accompanying power amplifier. Considering a Permanent Magnet Synchronous Motor (PMSM) and its accompanying Power Amplifier (PA) as one object, the strict control law using traditional sliding-surface reaching speed and additional exponential components has created the anti-disturbance torque control signal for the system. Synthesis of the sliding mode controller is guaranteed mathematically based on Lyapunov stability. The disturbance compensation control component is quantified based on the upper and lower bounds of disturbance. Simulation in Matlab shows visual research findings.**

***Index Terms*—PMSM tracking drive system, strict sliding mode control, power reaching law, Lyapunov stability, disturbance bounds**

I. Introduction

Currently, due to its stiff torque characteristics with wide speed variation, many traction drive systems have been using Permanent Magnet Synchronous Motors (PMSM) with Power Amplifiers (PA) or inverters [1−5]. This application-oriented approach facilitates the design and synthesis of control systems by exploiting the basic PMSM motor control algorithms and methods already built into the PA [6−10]. However, in high-quality tracking systems such as aerial target tracking systems and element-firing tracking systems [11], because they operate in transient mode, the primary control algorithms integrated inside the PA alone do not guarantee the tracking quality of the system. This contradiction raises a scientific problem, the need for suitable outer-loop controllers. Although in some studies such as [4, 5], system designers have synthesized controllers such as PI, PIV, PIDV, or gain scheduling. However, when the reference speed signal changes, it is still necessary to have subjective controlling parameter adjustments, limiting the system's adaptability.

Variable Structural Control (VSC) and Sliding Mode Control (SMC) were proposed by Utkin, Itkis, and Emelyanov. Over the decades, VSC and SMC have been interested in research by the academic community and are increasingly enriching and deepening [12−15]. SMC is currently being applied as a general design solution for many control systems, such as linear systems, nonlinear systems, systems with multiple inputs and outputs (MIMO), or discrete and random systems [16−19]. The advantage of SMC is that when in sliding mode, the system is not sensitive to parameter uncertainty and disturbance, so the stability of the control system is guaranteed [13−15].

This study considered the PMSM actuator and PA as the control object, but it differs from the studies [1−5] where the PA-PMSM adjustment is in position control mode. The article proposes a new approach whereby the PA is adjusted to work with the PMSM in the combined position-torque mode. This synthesis takes advantage of the precise resolution of the position control mode. It facilitates the control law of the outer loop by direct-torque control through a DC voltage input. With this object, the outer loop sliding control law is synthesized based on the combination of constant sliding-surface reaching speed and exponential reaching speed [2, 3], [20−24]. The disturbance compensation control component is quantified based on the upper bound and lower bound of the disturbance, so the constant sliding-surface reaching speed is strictly confined.

The paper is organized as follows: After the introduction section, the second one presents the state space equation of the control object (PA-PMSM). The third section synthesizes the strict sliding mode controller and proves the system's stability. The fourth section presents simulation results. Finally, there are some conclusions given.

II. State-Space Equation of PA-PMSM

The traction drive system using the PA-PMSM actuator is currently a technology trend, and the actual hardware configuration has been studied and applied by many studies.

The PMSM mechanical motion equation dynamics equation [1, 2]:

$$J_m\ddot{\theta} = M_m - M_L - b\dot{\theta} \quad (1)$$

where $\ddot{\theta}$ and $\dot{\theta}$ are the angular acceleration and the actual angular speed relative to the motor shaft end, b is

Manuscript received January 10, 2023; revised March 12, 2023; accepted May 24, 2023.

the coefficient of viscous friction (which depends on the rotational speed), M_m is the electromagnetic torque - the motor shaft end torque (torque control signal), M_L is the time-varying load torque (disturbance), and J_m is the inertia moment of the motor.

When the PA is set to the combined position and torque control mode, the control signal input to the PA is a DC voltage signal u_v. The outer loop controller synthesizes the voltage control signal u_v. The PA takes care of the imposition of torque on the motor shaft.

Using the pre-set current control loop, the PA will operate in direct torque control mode, and the kinematics of the PA-PMSM block has the form of the torque multiplied by the control voltage [6].

$$M_m = k_m u_v \tag{2}$$

where k_m is the torque adjustment coefficient.

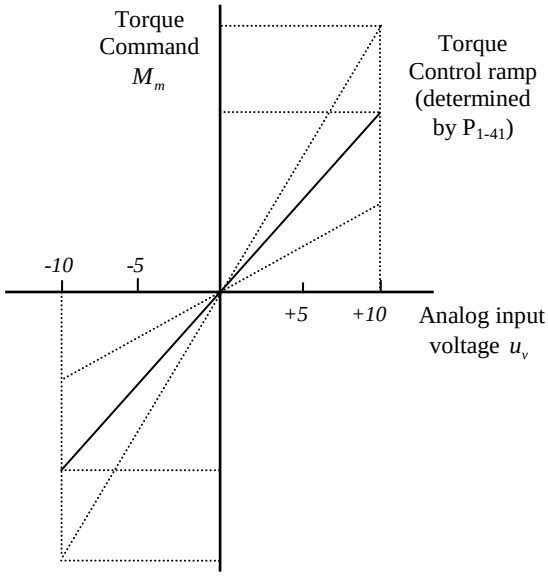

Fig. 1. Direct torque control characteristics of Delta.

Fig. 1 shows the torque control characteristics of Delta's PA, determined by parameter P1-41 [25]. This parameter is to set the maximum analog torque command corresponding with the maximum input voltage $u_v = [-10; +10]V$. For example, if P1-41 equals 100 and the input voltage is +10V, it indicates that the torque command is 100% rated torque. If P1-41 equals 100, but the input voltage changes to +5V, then the torque command is changed to 50% rated torque. Suppose the limit of rated torque is $M_{\max}$, then:

$$M_m = \frac{M_{\max} P_{1-41}}{10} u_v \tag{3}$$

Set the angular tracking error and the derivative of the tracking error as Eq. (4):

$$e = \theta_d - \theta;\ \dot{e} = \dot{\theta}_d - \dot{\theta} \tag{4}$$

where θ is the actual angle; θ_d is the desired angle.

Combining Eq. (1), Eq. (2), and Eq. (4), the dynamics equation of the PA-PMSM object is:

$$-J_m\ddot{e} - b\dot{e} - k_m u_v + J_m\ddot{\theta}_d + b\dot{\theta}_d + M_L = 0 \tag{5}$$

Setting $x_1 = e; x_2 = \dot{e}$ in Eq. (5), we get the state space:

$$\begin{cases} \dot{x}_1 = x_2 \\ \dot{x}_2 = -\dfrac{b}{J_m} x_2 - \dfrac{k_m}{J_m} u_v + \left(\ddot{\theta}_d + \dfrac{b}{J_m}\dot{\theta}_d + \dfrac{M_L}{J_m} \right) \end{cases} \tag{6}$$

III. Strict Sliding Mode Control with Power Reaching Law and Disturbance Bounds

Choose a sliding surface Eq. (7):

$$S = \lambda x_1 + x_2 = 0;\ \lambda > 0 \tag{7}$$

Take the first derivative of the sliding function and combine it with the state space Eq. (6):

$$\begin{aligned} \dot{S} &= \lambda\dot{x}_1 + \dot{x}_2 = \lambda x_2 + \dot{x}_2 \\ &= \left(\lambda - \frac{b}{J_m} \right) x_2 - \frac{k_m}{J_m} u_v + \left(\ddot{\theta}_d + \frac{b}{J_m}\dot{\theta}_d + \frac{M_L}{J_m} \right) \end{aligned} \tag{8}$$

The sliding-surface power reaching law and exponential reaching law was used in several studies [1, 3], [20−24]. In a traditional sliding mode controller with exponential reaching law, fast reaching and low chattering cannot be considered simultaneously. In [1], the continuous symmetric S-type function instead of the sign function and the combined exponential and power reaching laws were introduced. However, power components were used in all terms for reaching laws with a higher degree of S-type function. In [3, 23, 24], the basic sliding-surface reaching law with constant speed and the sliding-surface power reaching law were also proposed. These works offered a combined sliding-surface reaching law Eq. (9) and discussed stricter conditions for constant sliding-surface reaching speed ε.

Based on the conventional exponential reaching law [20], the paper proposed the power reaching laws with one power term in S to get more straightforward solutions and stricter disturbance conditions. This reaching law increases the sliding-surface reaching speed when the system states are far from the sliding surface; reduces the reaching rate when the system states are close to the sliding surface. As a result, the system quickly enters sliding mode and significantly limits chattering.

$$\dot{S} = -\varepsilon \operatorname{sgn}(S) - k|S|^{\alpha} \operatorname{sgn}(S),\ \varepsilon > 0;\ k > 0;\ 1 > \alpha > 0 \tag{9}$$

From Eq. (8) and Eq. (9), homogeneously, we get the equation:

$$\begin{aligned} &\left(\lambda - \frac{b}{J_m} \right) x_2 - \frac{k_m}{J_m} u_v + \left(\ddot{\theta}_d + \frac{b}{J_m}\dot{\theta}_d + \frac{M_L}{J_m} \right) \\ &= -\varepsilon \operatorname{sgn} S - k|S|^{\alpha} \operatorname{sgn}(S) \end{aligned} \tag{10}$$

From Eq. (10), get the controller Eq. (11) as follows:

$$u_v = \frac{1}{k_m}\left[\left(\lambda J_m - b\right)x_2 + \varepsilon J_m \operatorname{sgn}\left(S\right)\right] + \frac{k}{k_m} J_m |S|^{\alpha} \operatorname{sgn}\left(S\right) + \frac{1}{k_m}\left(J_m \ddot{\theta}_d + b\dot{\theta}_d + M_L\right) \quad (11)$$

Because M_L is the bounded uncertainty load disturbance, that is $M_1 \le M_L \le M_2$, the controller Eq. (11) will be proposed by the controller Eq. (12).

$$u_v = \frac{1}{k_m}\left[\left(\lambda J_m - b\right)x_2 + \varepsilon J_m \operatorname{sgn}\left(S\right)\right] + \frac{k}{k_m} J_m |S|^{\alpha} \operatorname{sgn}\left(S\right) + \frac{1}{k_m}\left(J_m \ddot{\theta}_d + b\dot{\theta}_d - \bar{M}\right) \quad (12)$$

The following theorem shows the conditions for the disturbance compensation component $\bar{M}$ and stricter conditions for constant sliding-surface reaching speed ε.

Theorem: The controller Eq. (12) with the sliding surface Eq. (7) and sliding-surface reaching law Eq. (9) ensures the control system Eq. (6) exists in sliding mode, and the system states $x_1, x_2 \to 0$ with conditions:

$$\bar{M} = -\frac{M_2 + M_1}{2} + \frac{M_2 - M_1}{2}\operatorname{sgn}\left(S\right);\ \varepsilon \ge \frac{M_2 - M_1}{J_m} \quad (13)$$

where M_1 and M_2 are, respectively, the lower and upper bounds of disturbance M_L.

Proof.

a) Exist of sliding mode

Choose a Lyapunov function of the form Eq. (14):

$$V = \frac{1}{2}S^2 \quad (14)$$

The derivative V to time:

$$\dot{V} = S\dot{S} \quad (15)$$

Here we find the conditions for $\dot{V} < 0$. It is necessary to consider the kinematics of the sliding surface S. We need to consider the derivative of the sliding surface S.

Substitute Eq. (12) into the second equation of Eq. (6):

$$\dot{x}_2 + \lambda x_2 = -\varepsilon \operatorname{sgn}\left(S\right) - k|S|^{\alpha} \operatorname{sgn}\left(S\right) + \frac{M_L + \bar{M}}{J_m}$$
$$\dot{S} = -\varepsilon \operatorname{sgn}\left(S\right) - k|S|^{\alpha} \operatorname{sgn}\left(S\right) + \frac{M_L + \bar{M}}{J_m} \quad (16)$$

Taking $\dot{S}$ from Eq. (16) into Eq. (15), we have

$$\dot{V} = -\varepsilon S \operatorname{sgn}\left(S\right) - k|S|^{\alpha} S \operatorname{sgn}\left(S\right) + \frac{M_L + \bar{M}}{J_m} S$$
$$= \frac{M_L + \bar{M}}{J_m} S - \varepsilon|S| - k|S|^{\alpha+1} \quad (17)$$
$$= \dot{V}_1 - k|S|^{\alpha+1}$$

where

$$\dot{V}_1 = \frac{M_L + \bar{M}}{J_m} S - \varepsilon|S| \quad (18)$$

Replace $\bar{M}$ from the assumption in Eq. (18):

$$\dot{V}_1 = \frac{2M_L - M_2 - M_1 + \left(M_2 - M_1\right)\operatorname{sgn}\left(S\right)}{2J_m} S - \varepsilon S \quad (19)$$

To have $\dot{V} < 0$, we need to prove $\dot{V}_1 \le 0$ with the conditions (assumptions) of the theorem. There are 3 cases according to S as follows:

1) When $S = 0$*:*

$$\dot{V}_1 = 0 \quad (20)$$

2) When $S > 0$*:*

$$\dot{V}_1 = \left(\frac{M_L - M_1}{J_m} - \varepsilon\right) S \quad (21)$$

According to the assumption: $\varepsilon \ge \left(M_2 - M_1\right)/J_m$, and because of $M_2 > M_L$, so:

$$\varepsilon \ge \frac{M_2 - M_1}{J_m} > \frac{M_L - M_1}{J_m} \quad (22)$$

That means:

$$\frac{M_L - M_1}{J_m} - \varepsilon < 0 \Rightarrow \dot{V}_1 < 0 \quad (23)$$

3) When $S < 0$*:*

$$\dot{V}_1 = \left(\varepsilon - \frac{M_2 - M_L}{J_m}\right) S \quad (24)$$

According to the assumption: $\varepsilon \ge \left(M_2 - M_1\right)/J_m$, and because of $M_1 < M_L$, so:

$$\varepsilon \ge \frac{M_2 - M_1}{J_m} > \frac{M_2 - M_L}{J_m} \quad (25)$$

That means:

$$\varepsilon - \frac{M_2 - M_L}{J_m} > 0 \Rightarrow \dot{V}_1 < 0 \quad (26)$$

From Eq. (20), Eq. (23) and Eq. (26) we have $\dot{V}_1 \le 0\ \forall S$ so $\dot{V} = \dot{V}_1 - k|S|^{\alpha+1} \le 0\ \forall S$ and V is bounded, S is also limited.

The conditions $\dot{V} \le 0\ \forall S$ only ensure that $\dot{V}$ is a negative semi-deterministic function, so V cannot be an actual Lyapunov function yet.

Without loss of generality, consider M_L to be a slowly varying disturbance, then:

$$\frac{dM_L}{dt} \approx 0;\ \frac{d\bar{M}}{dt} = 0 \quad (27)$$

From Eq. (17), calculate the second derivative of V, and use Eq. (27) to get $\ddot{V}$:

$$\ddot{V} = \varepsilon^2 + \varepsilon k|S|^{\alpha} + \varepsilon k(\alpha+1)|S|^{\alpha}\operatorname{sgn}(S) + k^2(\alpha+1)|S|^{2\alpha}\operatorname{sgn}(S) - \frac{\varepsilon(\bar{M}+M_L)}{J_m}\operatorname{sgn}(S) - \frac{k(\bar{M}+M_L)}{J_m}|S|^{\alpha}\operatorname{sgn}(S) - \frac{(\bar{M}+M_L)^2}{J_m} \quad (28)$$

Eq. (28) shows that $\ddot{V}$ is a function of S. Because S is continuous and bounded, so $\dot{V}$ is also bounded and $\dot{V}$ is a uniformly continuous function. Barbalat lemma guarantees that

$$\dot{V} = \frac{M_L + \bar{M}}{J_m}S - \varepsilon|S| - k|S|^{\alpha+1} \to 0 \Rightarrow S \to 0 \quad (29)$$

So, controller Eq. (12) ensures that system Eq. (6) exists in sliding mode.

b) System states $x_1, x_2 \to 0$

When the system exists in sliding mode, $S = 0$:

$$S = \lambda x_1 + x_2 = \lambda x_1 + \dot{x}_1 = 0 \Leftrightarrow \lambda x_1 = -\dot{x}_1 \Leftrightarrow \ln|x_1| = -\frac{1}{\lambda}t + C \quad (30)$$

where C is a constant.

Assume the system states at the time of falling on the sliding surface: $x_{1s}|_{t=t_0} = x_{1s}(t_0)$, then:

$$C = \ln|x_{1s}(t_0)| + \frac{1}{\lambda}t_0 \quad (31)$$

Combine Eq. (30) and Eq. (31) to get:

$$\ln|x_1| = -\frac{1}{\lambda}t + \ln|x_{1s}(t_0)| \quad (32)$$

$$x_1 = x_{1s}(t_0)e^{-\frac{1}{\lambda}(t-t_0)}, \quad x_2 = -\frac{x_{1s}(t_0)}{\lambda}e^{-\frac{1}{\lambda}(t-t_0)} \quad (33)$$

Because of $\lambda > 0$ so, the formula Eq. (33) shows that $x_1, x_2 \to 0$ as $t \to \infty$. Thus, the controller Eq. (12) guarantees that the system states $x_1, x_2 \to 0$. The theorem has been proved.

***Remark**:* The disturbance parameter M_L varies in the range $[M_1; M_2]$. The theorem shows the stricter conditions of ε , which:

$$\varepsilon \geq (M_2 - M_1)/J_m \quad (34)$$

IV. Simulation Results

Consider the system Eq. (35) under the influence of the disturbance Eq. (36) [12] with the profile graph in Fig. 2.

$$\ddot{\theta} = -25\dot{\theta} + 133u_v - M_L \quad (35)$$

$$M_L = 50\exp\left[-\frac{(t-1.5)^2}{2\times 0.2^2}\right] - 20\exp\left[-\frac{(t-3)^2}{2\times 0.1^2}\right] \quad (36)$$

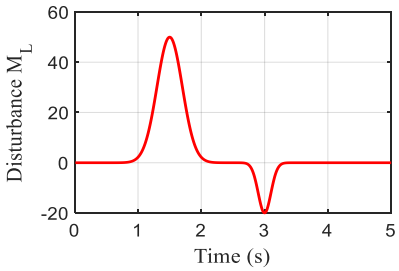

Fig. 2. Disturbance profile graph.

In Fig. 2: $M_1 = -20$; $M_2 = 50 \Rightarrow \bar{M} = -15 + 35\operatorname{sgn}(S)$.

Angular tracking error and its derivative:

$$e = \theta_d - \theta;\ \dot{e} = \dot{\theta}_d - \dot{\theta} \quad (37)$$

Setting $x_1 = e; x_2 = \dot{e}$, the system Eqs. (35−37), can be as Eq. (38):

$$\begin{cases} \dot{x}_1 = x_2 \\ \dot{x}_2 = -25x_2 - 133u_v + (\ddot{\theta}_d + 25\dot{\theta}_d + M_L) \end{cases} \quad (38)$$

Let us say angular position and initial angular speed:

$$\theta_d(0) = -0.5\text{rad};\ \dot{\theta}_d(0) = -0.5\text{rad/s} \quad (39)$$

With the desired angle as a step function $\theta_d = 1(t)$, the initial states of the system are:

$$[x_1 \quad x_2]^T = [1.5 \quad 0.5]^T \quad (40)$$

Set parameters for the controller:

$$\lambda = 15;\ \varepsilon = 70;\ \alpha = 0.8;\ k = 20 \quad (41)$$

The sliding surface has the form Eq. (42):

$$S = 15x_1 + x_2 = 0 \quad (42)$$

The sliding-surface reaching law has the form Eq. (43):

$$\dot{S} = -70\operatorname{sgn}(15x_1 + x_2) - 20|15x_1 + x_2|^{0.8}\operatorname{sgn}(15x_1 + x_2) \quad (43)$$

With $\theta_d = \sin(t)$, the controller has the form Eq. (44).

$$u_v = \frac{1}{133}\{20(15x_1 + x_2)^{0.8}\operatorname{sgn}(15x_1 + x_2) + 70\operatorname{sgn}(15x_1 + x_2) - 10x_2 - \sin(t) + 25\cos(t) + 15 - 35\operatorname{sgn}(15x_1 + x_2)\} \quad (44)$$

With $\theta_d = 1(t)$, the controller has the form Eq. (45):

$$u_v = \frac{1}{133}\{20(15x_1 + x_2)^{0.8}\operatorname{sgn}(15x_1 + x_2) + 70\operatorname{sgn}(15x_1 + x_2) - 10x_2 + 15 - 35\operatorname{sgn}(15x_1 + x_2)\} \quad (45)$$

***Case 1:* Simulation with $\varepsilon = 70$.**

Remark: There is chattering with the control signals in Fig. 3 (a) and Fig. 4 (a). Simulations performed with inputs 1(t) and sin(t) show that the system exists in sliding mode and the system states $\to 0$, as shown in Fig. 3 (b) and Fig. 4 (b). Desired and actual angles fit in Fig. 5 (a) and Fig. 5 (b). Note that the transient system time T_s = 0.5 s in Fig. 5 (b); load disturbance M_L is fully compensated with an angular tracking error, not exceeding 0.005 rad during the disturbance.

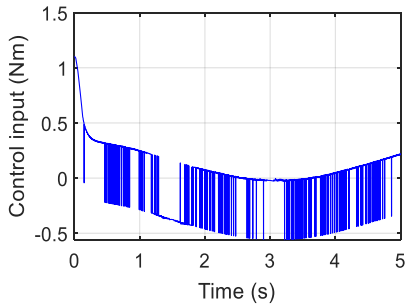

(a) Control signal

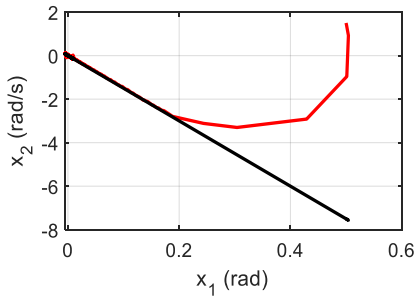

(b) System states

Fig. 3. Control signal and system state trajectory with $\theta_d = \sin(t)$.

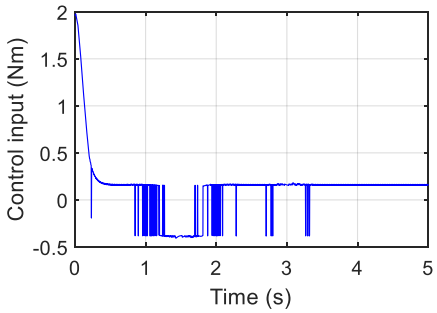

(a) Control signal

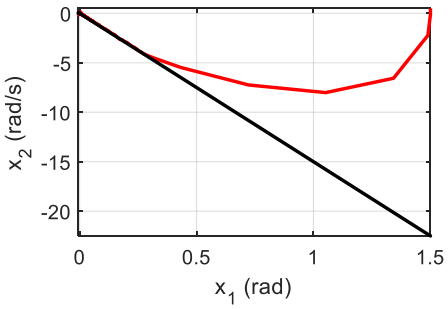

(b) System states

Fig. 4. Control signal and system state trajectory with $\theta_d = 1(t)$.

Fig. 3 and Fig. 4 show the state variables and control signal of the system. Although there is some chattering, the phase's trajectory converges to zero. Fig. 5 (b) shows a good system response with 0.5 second settling time. Actual angle tracked tightly desired angle (Fig. 5(a)).

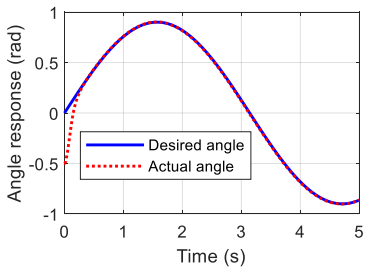

(a) System response to $\theta_d = \sin(t)$

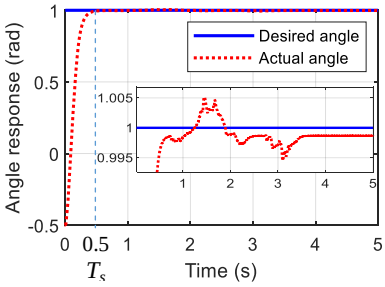

(b) System response to $\theta_d = 1(t)$

Fig. 5. System response to different inputs.

The case $\varepsilon = 70$ satisfies the conditions Eq. (13) of the theorem ($\varepsilon \geq 70$).

***Case 2:* Simulation with $\varepsilon = 60$**

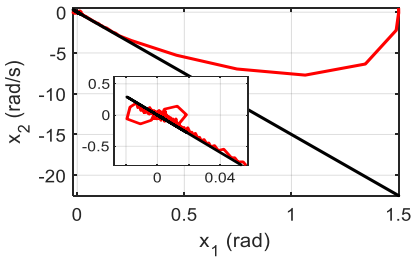

(a) System states

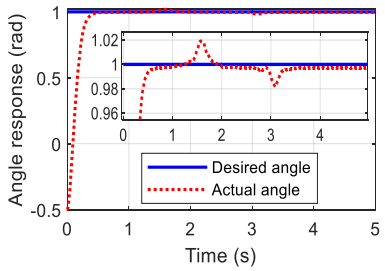

(b) System response

Fig. 6. Response and system states with $\theta_d = 1(t)$ and $\varepsilon = 60$.

Remark: Fig. 6 shows the phase trajectory and step response of the system. The system exists in sliding mode; the system states $\to 0$, but when the load disturbance M_L occurs, Fig. 6 (b) shows that the amount of disturbance compensation is not enough to keep the system in equilibrium; the system is knocked out of equilibrium states (Fig. 6 (a)) by disturbance, then slowly returns to equilibrium. In Fig. 6 (b), the load disturbance appears

when t_1 = 1.5 s and t_1 = 3.0 s visually represents this process. The reason is that the condition ε = 60 does not satisfy the condition $\varepsilon \geq 70$ that the theorem states.

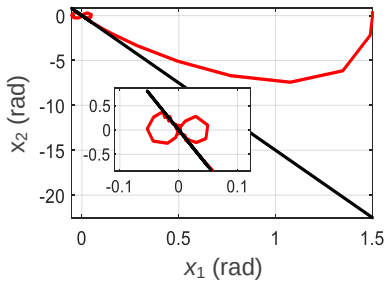

(a) System states

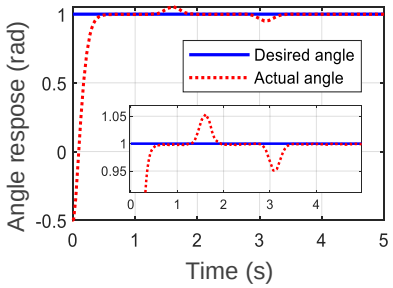

(b) System response

Fig. 7. Response and system states with $\theta_d = 1(t)$ and $\varepsilon = 50$.

Case 3: **Simulation with** $\varepsilon = 50$.

Remark: Fig. 7 shows the phase trajectory and step response of the system. The system exists in sliding mode; the system states $\to 0$, but when the load disturbance M_L occurs, Fig. 7 (b) shows that the amount of disturbance compensation is insufficient to keep the system in equilibrium. The system is knocked out of equilibrium states (Fig. 7 (a)) by disturbance, then slowly returns to equilibrium. The reason is that the condition $\varepsilon = 50$ does not satisfy the condition $\varepsilon \geq 70$ the theorem states. Compared with the case of $\varepsilon = 60$ (Fig. 6 (b)), the amount of disturbance compensation control when $\varepsilon = 50$ (Fig. 7 (b)) is less, so the system is thrown further from equilibrium.

Case 4: **Simulation with** $\varepsilon = 70;\ \alpha = 0.08;\ k = 220$.

Case 5: **Simulation with** $\varepsilon = 70;\ \alpha = 0.05;\ k = 225$.

Fig. 8 and Fig. 9 show the step response and the control signal u_v of the system in Case 4 and Case 5. The purpose of these two simulations is to keep the ε satisfying condition Eq. (34) and only adjust the power coefficient α and k factor to ensure better control quality and get low chattering.

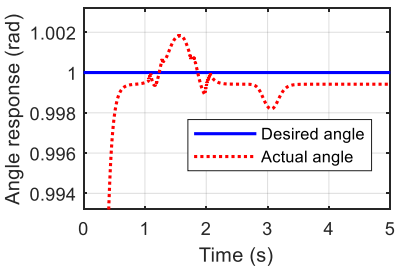

(a) System response to $\theta_d = 1(t)$

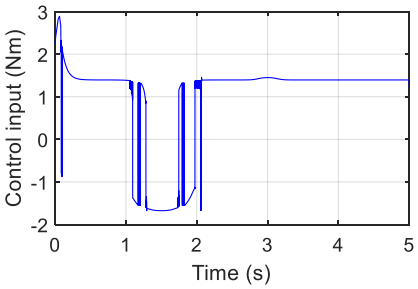

(b) Control signal

Fig. 8. Response and control input with $\theta_d = 1(t)$ and $\varepsilon = 70;\ \alpha = 0.08;\ k = 220$.

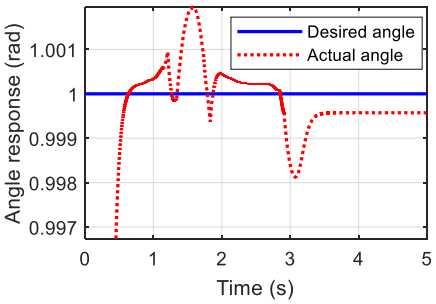

(a) System response to $\theta_d = 1(t)$

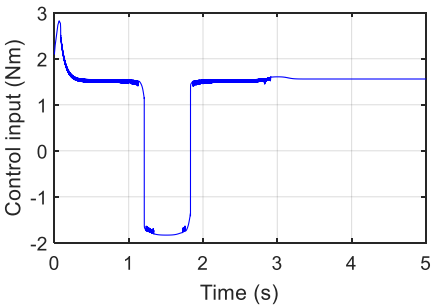

(b) Control signal

Fig. 9. Response and control input with $\theta_d = 1(t)$ and $\varepsilon = 70;\ \alpha = 0.05;\ k = 225$.

Remarks: In cases 4 and 5, simulations were conducted with ε = 70, but α and k changed to eliminate chattering.

With ε = 70, the tracking quality of the system was kept well in both Case 4 and Case 5 (Fig. 8 (a) and Fig. 9 (a)). However, the chattering phenomenon in Case 5 was better eliminated than it in Case 4 because the power reaching parameter α and the coefficient k multiplied to $|S|^{\alpha}\,\mathrm{sgn}(S)$ were tuned better (Fig. 8 (b) and Fig. 9 (b)).

In conclusion, simulation results show that:

1) Choosing the right ε not only helps the system to fall into the sliding mode quickly but also ensures to keep the system is in equilibrium when there is a change in the load disturbance M_L. If choosing the stricter ε, the more stringent the equilibrium of the system is kept and the better the tracking quality of the system.

2) Tuning α and k make the system eliminate the chattering phenomenon.

3) Controllers Eq. (44), Eq. (45) with sliding-surface reaching law Eq. (43) put the system in sliding mode and ensure the system states converge to zero.

V. Conclusion

The article presents a novel approach when considering the control object using the PMSM motor actuator and its accompanying PA in the combined position-torque mode. This approach facilitates the synthesis of the law of direct control of the outer loop torque through a DC voltage input. Still, it takes advantage of the high-resolution characterization of the position control mode. This study has synthesized the outer-loop sliding mode control law for the angle tracking system with stricter conditions of the constant sliding-surface reaching speed component ε. The solution that combines the sliding surface reaching-speed components has ensured the adaptability and sustainability of the system. Research results are proven mathematically and simulated intuitively.

Conflict of Interest

The authors declare no conflict of interest.

Acknowledgment

The authors gratefully acknowledge the reviewers' constructive and insightful comments to improve this paper's quality further. This work was supported in part by a grant from CAPITI.

References

[1] L. Yu, B. X. Hu, and K. Y. Wei, *Modern Permanent Magnet Synchronous Motor Control Principle and MATLAB Simulation*, 1st ed.; Beijing University of Aeronautics and Astronautics Press: Beijing, China, pp. 4–55, 2016. https://doi.org/10.3390/en14217293

[2] J. Lin, Y. Zhao, P. Zhang, J. Wang, and H. Su, "Research on compound sliding mode control of a permanent magnet synchronous motor in electromechanical actuators," *Energies*, vol. 14, no. 21, #7293, 2021. https://doi.org/10.3390/en14217293

[3] C. Qu, Y. Hu, Z. Guo, F. Han, and X Wang, "New sliding mode control based on tracking differentiator and RBF neural network," *Electronics*, vol. 11, no. 19, #3135, 2022. https://doi.org/10.3390/electronics11193135

[4] K. Suman and A. T. Mathew, "Speed control of permanent magnet synchronous motor drive system using P.I., PID, SMC and SMC plus PID controller," in *Proc. of 2018 Int. Conf. on Advances in Computing, Communications and Informatics*, 2018, pp. 543-549.

[5] R. I. Sudjoko, Hartono, and P. Iswahyudi, "Speed control of permanent magnet synchronous motor using universal bridge and PID controller," in *Proc. of the 6th Int. Conf. and Exhibition on Sustainable Energy and Advanced Materials*, Lecture Notes in Mechanical Engineering. Springer, Singapore, 2020. https://doi.org/10.1007/978-981-15-4481-1_39

[6] K. David, "Fundamentals of servo motion control," *Parker Compumotor*, 2007.

[7] X. Liu, Y. Pan, Y. Zhu, H. Han, and L. Ji, "Decoupling control of permanent magnet synchronous motor based on parameter identification of fuzzy least square method," *Progress in Electromagnetics Research M*, vol. 103, pp. 49-60, 2021. https://doi.org/10.2528/PIERM21032601

[8] Z. Wu, W. Gu, Y. Zhu, and K. Lu, "Current control methods for an asymmetric six-phase permanent magnet synchronous motor," *Electronics*, vol. 9, no. 1, #172, 2020.

[9] G. Liao, W. Zhang, and C. Cai, "Research on a PMSM control strategy for electric vehicles," *Advances in Mechanical Engineering*, vol. 13, no. 12, 2021. https://doi.org/10.1177/16878140211051462

[10] M. Tian, K. Wang, H. Lv, and W. Shi, "Reinforcement learning control method of torque stability of three-phase permanent magnet synchronous motor," *J. Phys.: Conf, Ser.*, vol. 2183, #012024, 2022. http://doi.org/10.1088/1742-6596/2183/1/012024

[11] H. Q. Vũ and B. N. Trần, "Synthesis of an improved fast terminal sliding mode controller for opto-electronic observatory in mobile vehicle," *International Journal of Electrical and Electronic Engineering & Telecommunications*, vol. 9, no. 6, pp. 434-440, 2020.

[12] V. Q. Huy and T. N. Binh, "Adaptive terminal sliding mode control by identifying uncertain and mutated disturbance with reference model," *J. Electr. Eng. Technol.*, vol. 15, pp. 1789–1796, 2020. https://doi.org/10.1007/s42835-020-00432-7.

[13] T. R. Oliveira, J. P. V. S. Cunha, and L. Hsu, "Adaptive sliding mode control based on the extended equivalent control concept for disturbances with unknown bounds," *Studies in Systems, Decision and Control*, vol 115. Springer, Cham, 2018. https://doi.org/10.1007/978-3-319-62896-7_6.

[14] S. Roy, S. Baldi, and L. M. Fridman, "On adaptive sliding mode control without a priori bounded uncertainty," *Automatica*, #108650, 2019. https://doi.org/10.1016/j.automatica2019.108650

[15] L. Ibarra, A. Rosales, P. Ponce, and A. Molina, "Adaptive SMC based on the dynamic containment of the sliding variable," *Journal of the Franklin Institute*, 2020. https://doi.org/10.1016/j.jfranklin.2020.12.005

[16] J. Zhang, D. Shi, and Y. Xia, "Design of sliding mode output feedback controllers via dynamic sliding surface," *Automatica*, #109310, 2020. https://doi.org/10.1016/j.automatica.2020.109310

[17] Y. Chen, C. Jiang, J. Dong, and Z. Zhao, "Output feedback sliding mode control based on adaptive sliding mode disturbance observer," *Measurement and Control*, 2022. https://doi.org/10.1177/00202940221114491

[18] Y. L. Yeh, "Output feedback tracking sliding mode control for systems with state- and input-dependent disturbances," *Actuators*, vol. 10, no. 6, #117, 2021. https://doi.org/10.3390/act10060117

[19] D. Shi, J. Zhang, Z. Sun, *et al*., "Adaptive sliding mode disturbance observer-based composite trajectory tracking control for robot manipulator with prescribed performance," *Nonlinear Dyn.*, vol. 109, pp. 2693–2704, 2022. https://doi.org/10.1007/s11071-022-07569-2

[20] Y. Wang, Y. Feng, X. Zhang, J. Liang, and X. Cheng, "New reaching law control for permanent magnet synchronous motor with extended disturbance observer," *IEEE Access*, vol. 7, pp. 186296-186307, 2019.

[21] C. Xiu, L. Yuan, and J. Li, "A new exponential power combined reaching law sliding-mode control for permanent magnet synchronous motor," in *Proc. 33rd Chinese Control and Decision Conf. (CCDC)*, 2021, pp. 230-235.

[22] S. Benzaouia, N. M'Sirdi, A. Rabhi, and A. Naamane, "Integral sliding mode control with exponential reaching law for PMSM in electric vehicles," *IFAC-Papers Online*, vol. 12, no. 55, pp. 222-227, 2022.

[23] S. Li, H. Wang, H. Li, and C. Yang, "PMSM sliding mode control based on novel reaching law and extended state observer," *Advances in Mechanical Engineering*, vol. 14, no. 8, pp. 1–16, 2022. https://doi.org/10.1177/16878132221119960.

[24] D. Zhang, T. Wu, S. Shi, and Z. Dong, "A modified active disturbance-rejection control with sliding modes for an uncertain system by using a novel reaching law," *Electronics*, vol. 11, #2392. 2022. https://doi.org/10.3390/electronics11152392

[25] Delta Standard AC Servo Drive for General Purpose Application—ASDA-B2 Series User Manual. [Online]. Available: https://www.cnc-steuerung.com/media/pdf/0e/5a/10/B2_Manual_ASDA-B2qOwicUaOSJb8l.pdf

Quoc Huy Vu received a B.S. degree in automation from Hanoi University of Science and Technology, Vietnam, in 2003 and a Ph.D. in control engineering and automation from the Academy of Military Science and Technology, Vietnam, in 2018. Since 2003 he has been a researcher at Control, Automation in Production and Improvement of Technology Institute (CAPITI), Hanoi, Vietnam. His research interests include intelligent control, robotic control systems and tracking systems in moving vehicles.